Experimental investigation of the detection mechanism in WSi nanowire superconducting single photon detectors

Rosalinda Gaudio᾽ , Jelmer J. Renema᾽ , Zili Zhou, Varun B. Verma, Adriana E. Lita, Jeffrey Shainline, Martin J. Stevens, Richard P. Mirin, Sae Woo Nam, Martin P. van Exter, Michiel J. A. de Dood, and Andrea Fiore

Experimental investigation of the detection mechanism in WSi nanowire superconducting single photon detectors

Rosalinda Gaudio,[1,a),b)] Jelmer J. Renema,[2,a),c)] Zili Zhou,[1] Varun B. Verma,[3] Adriana E. Lita,[3] Jeffrey Shainline,[3] Martin J. Stevens,[3] Richard P. Mirin,[3] Sae Woo Nam,[3] Martin P. van Exter,[2] Michiel J. A. de Dood,[2] and Andrea Fiore[1]

[1]COBRA Research Institute, Eindhoven University of Technology, P.O. Box 513, 5600MB Eindhoven, The Netherlands
[2]Huygens-Kamerlingh Onnes Laboratory, Leiden University, Niels Bohrweg 2, 2333CA Leiden, The Netherlands
[3]National Institute of Standards and Technology, 325 Broadway, Boulder, Colorado 80305, USA

We use quantum detector tomography to investigate the detection mechanism in WSi nanowire superconducting single photon detectors. To this purpose, we fabricated a 250 nm wide and 250 nm long WSi nanowire and measured its response to impinging photons with wavelengths ranging from $\lambda = 900$ nm to $\lambda = 1650$ nm. Tomographic measurements show that the detector response depends on the total excitation energy only. Moreover, for total absorbed energies >0.8 eV the current–energy relation is linear, similar to what was observed in NbN nanowires, whereas the current–energy relation deviates from linear behavior for total energies below 0.8 eV. *Published by AIP Publishing.*
[http://dx.doi.org/10.1063/1.4958687]

Nanowire superconducting single photon detectors (SSPDs)[1] are a key technology for the development of quantum communication and computation.[2] Their fast response time combined with their low dark count rate, low jitter, and single- and multi-photon counting capability favor the use of this technology in applications such as quantum key distribution (QKD),[3] quantum optics,[4] nanoscale imaging,[5] and interplanetary optical communication.[6]

The earliest SSPDs were made of polycrystalline films of NbN, NbTiN, and TaN, and different techniques were used to maximize optical coupling into the superconducting film.[2] Despite technological efforts, these detectors are still affected by low fabrication yield[7,8] and the highest system detection efficiency (SDE) reported for $\lambda = 1550$ nm is not higher than 80%.[9,10]

Recently, amorphous superconducting films have attracted the interest of the SSPD community.[11–14] Although operating at much lower temperatures, the advantage of SSPDs based on amorphous WSi[14] (and also MoSi[15] and MoGe[16]) is that their internal detection efficiency saturates close to unity[11] at currents well below the critical current. Due to their high internal detection efficiency, devices patterned from such films have an SDE higher than 90% (Ref. 14) and higher yield.[17] It is an open question whether these striking differences between NbN and WSi films are related to differences in the physics of the detection process.

For NbN SSPDs, we demonstrated[18,19] that the detection event is due to a vortex crossing induced by a cloud of quasi-particles, which reduces the potential barrier for vortex entry. The energy dissipated by the vortex crossing the nanowire leads to a transition to the normal state.[20–22] Contrary to early models,[23] we found that the detection event cannot be described by the local increase of current density over the critical value due to a photo-generated normal core hotspot.

For WSi, in contrast, little is known about the detection mechanism. Compared with NbN,[24–26] a typical[27] thin WSi film is characterized[28,29] by a higher normal-state electron diffusion coefficient of 0.75 cm²/s vs. 0.5 cm²/s, a larger coherence length (9 nm versus 4 nm), a lower superconducting gap (0.5 meV vs. 2 meV), and a lower density of states at the Fermi level (2×10^{22} eV^{-1}cm^{-3} vs. 4×10^{22} eV^{-1}cm^{-3}). According to simulations that take into account these properties, these differences are enough to lead to a qualitative change in the detection mechanism. Absorption of a single photon is expected to result in the formation of a normal hotspot, at wavelengths up to the mid-infrared.[29]

Moreover, pump-probe experiments on the two materials produce qualitatively different results. In WSi,[30] the lifetime of an excitation created by an absorbed photon is strongly dependent on bias current. In a bias current range from 0.45 to 0.65 I_b/I_c, the excitation lifetime changes by an order of magnitude. In contrast, in NbN,[31,32] the lifetime is constant over a similar range of bias currents (0.3–0.55 I_b/I_c).

For WSi, the two-photon behavior is governed by the recombination of quasiparticles.[33] In NbN, in contrast, quasiparticle multiplication and diffusion set the relevant timescales. Both experimental evidence[19,43] and theoretical calculations[29] point to a hotspot size of about 20–30 nm in diameter, which leads to an estimated detection time of 2–5 ps, much shorter than the QP recombination time. These results indicate substantial differences in the phenomenology of these materials.

In this work, we experimentally investigate the detection mechanism in WSi nanowire SSPDs. We use quantum detector tomography (QDT)[34,35] and multiphoton excitations[18] to measure the energy–current relation,[36,37] i.e., the amount of

---

bias current (I_b^{th}) required to produce a detection event with a fixed probability (1%) as a function of the detected energy (E_t). This functional dependence is a key signature of the detection mechanism.

We find linear scaling between photon energy and bias current at constant detection probability, similar to NbN. This scaling holds in the range $E_t = 0.8\,\text{eV}–2.25\,\text{eV}$, and we can parameterize it as $I_b^{th} = I_o - \gamma E_t$, with $\gamma = 1.7\,\mu\text{A/eV}$, $I_0/I_c = 0.7$, where I_c is the critical current of the device. As in NbN, we find that the current required to achieve a detection event only depends on the total energy of the photons participating in the detection event. We experimentally rule out the quadratic scaling which is expected from the original normal-core hot spot model[23] and from the simulations of Engel *et al.*[29] For energies $E_t \leq 0.8\,\text{eV}$, experimental data deviate from the linear relation. The strong similarity between our results and those obtained on NbN indicates—surprisingly—that the differences in material parameters do not substantially alter the phenomenological description of the detection mechanism.

Our device consists of 5 nm thick WSi, with a critical temperature of $T_c = 3.7\,\text{K}$, on a GaAs substrate.[38] The device is fabricated into a 250 nm wide, 250 nm long bridge using reactive ion etching and e-beam lithography (Figure 1). The sample is cooled to 1.6 K, and we observe a critical current of $9.4\,\mu\text{A}$. We have previously shown[18] for NbN that the current– energy relation is independent of the device geometry: the energy–current relation for a short bridge device is identical to that obtained with a meander. Furthermore, the position dependence of the detection efficiency inferred from such a device carries over to meander devices.[19]

The device is illuminated with a Fianium supercontinuum pulsed laser[39] with a repetition rate of 20 MHz, which provides a broadband spectrum from 600 nm to 1800 nm. The laser light is linearly polarized perpendicular to the nanowire longitudinal axis using polarization-maintaining components throughout. We use a lensed fiber to illuminate the device, which produces a beam spot with nominal diameter of $2.9\,\mu\text{m}$ at 1550 nm.

To measure the multiphoton response of our sample, we make use of quantum detector tomography (QDT).[34] The goal of QDT is to measure the probability of a detection event given that n photons are incident on a detector. This is done by recording the detection probability under illumination with coherent states. Since the coherent states form a (overcomplete) basis for the space of quantum states of light, this information is sufficient to infer the response of the device to Fock states (which is the desired quantity) by means of a basis transformation.

During each experimental run, we record the counts of the detector while varying the light power P and the bias current I_b. We perform this experiment independently at a series of wavelengths ($\lambda = 950\,\text{nm} - 1650\,\text{nm}$, $\Delta\lambda = 10 \pm 2\,\text{nm}$).

We make use of the modified protocol described in Ref. 35. In this description, the detection probability R as function of the input mean photon number N is given by

$$R(N) = \exp(-\eta N) \sum_{n=0}^{\infty} p_n \frac{(\eta N)^n}{n!}, \tag{1}$$
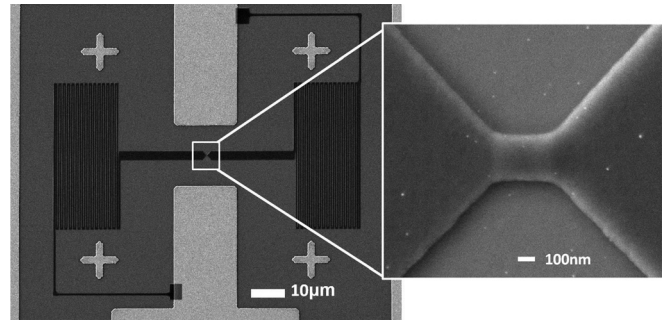
FIG. 1. Scanning electron microscope image of the WSi device. The magnification on the right shows the active area of a nanowire detector similar to that involved in the measurements.

where η is a parameter that captures all linear loss, and the parameter p_n measures the probability that n absorbed photons trigger a detection event. A minimal set of p_n that adequately describes the detector can be found by using a sparsity assumption.[35]

Figure 2 shows a typical data set for an experimental run at 1650 nm. The effective linear detection efficiency η and the internal detection probabilities p_1, p_2, and p_3 are plotted as a function of I_b. For $I_b > 5.5\,\mu\text{A}$ the device mostly detects single photons, while for $4\,\mu\text{A} < I_b < 5.5\,\mu\text{A}$ it detects predominantly two or more photons ($p_1 < 0.01$). The data for $I_b > 7\,\mu\text{A}$ are not considered since the corresponding pure single-photon regime does not contain any interesting dynamics.

The observed linear efficiency of $\eta \approx 5 \times 10^{-4}$ is consistent with the fraction of photons absorbed into the active area of our detector. The gradual decrease in efficiency at low bias currents could be due to the finite probability of overlap between the excitations along the length of the detector.[40,43] The small jumps in efficiency which occur at $I_b = 4\,\mu\text{A}$ and $I_b = 5.5\,\mu\text{A}$ are related to the different model (i.e., different number of fitting parameters) used in the different photon-number regimes. This is due to the limited ability of the protocol to resolve values of $p_n \gtrsim 0.3$ due to additional nonlinearities which occur at the high count rates required to resolve such values.[41]
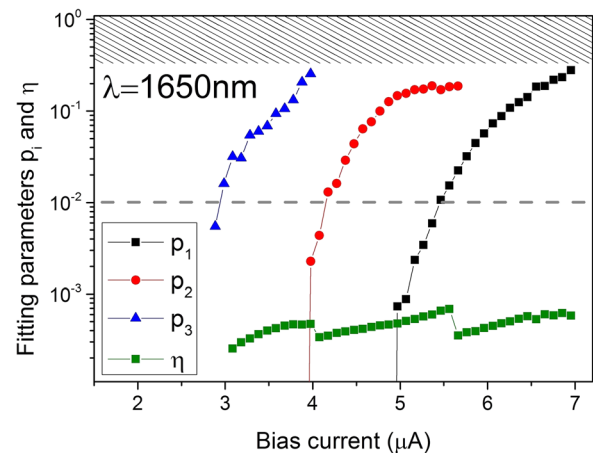
FIG. 2. The p_i and η displayed as a function of bias current for the case $\lambda = 1650\,\text{nm}$. The horizontal dashed line indicates the probability level equal to 0.01. The dashed area indicates the values of p_n which are not accessible without present measurement.

From the observed values of p_n as a function of bias current we construct the energy–current relation. We plot the bias current required to obtain a detection event with fixed probability (1%) as a function of the overall excitation energy $E_t = n\frac{hc}{\lambda}$, where n is the number and λ the wavelength of the photons corresponding to the p_n in question. The 1%-threshold criterion is chosen to be in the range where the imperfections discussed above do not affect our results.

Figure 3 shows that the detector responds only to the total excitation energy. Data points corresponding to different wavelengths and numbers of photons lie on the same line, indicating that only the overall excitation energy matters. This is evident from the overlap of two data points highlighted by the red dotted circle in Figure 3, corresponding to the detection of three photons with wavelength $\lambda = 1650\,\text{nm}$ and two photons with $\lambda = 1100\,\text{nm}$. We stress that this result is independent of the choice of threshold detection probability, up to a small linear shift, similar to NbN.[18] These results indicate that the detection probability only depends on the total number of photo-created quasi-particles, as was observed in NbN nanowires.[18]

The data reported in Figure 3 provide the energy–current relation for a WSi nanowire SSPD. For energies corresponding to $E_t > 0.8\,\text{eV}$, the data lie on a straight line, which is parameterized by $I_{th} = I_0 - \gamma E_t$, with $\gamma = 1.6\,\mu\text{A/eV}$ and $I_o = 6.5\,\mu\text{A} = 0.7I_c$ (black dashed line in Figure 3). A fit of linear behavior excluding points with $E_t < 0.8\,\text{eV}$ gives a significantly better fit ($\chi^2 = 20$) than one which includes low energies ($\chi^2 = 47$). We note that the experimental data are not well described by the expression $I_b^{th} = I_o - \gamma\sqrt{E_t}$ which characterizes the normal-core hot spot model, regardless of whether we consider the whole data set or only high energies. For NbN, we previously found a linear dependence, with $I_0 = 0.75I_c$ and $\gamma = 1.6\,\mu\text{A/eV}$ for a 220 nm wide

detector.[18] In the high energy range, our results are therefore—surprisingly—almost identical to those obtained for NbN.

However, as shown in the inset, the first three points deviate from this linear trend significantly (as much as 19σ for the lowest energy point). We did not observe this deviation in NbN in our previous experiment, which had the same lower energy bound as the present work.[18] It was pointed out previously[33,42,44] for NbN that such a deviation must be expected on physical grounds, since the linear $I_b^{th} - E_t$ relation cannot hold for $E \approx 0$ if $I_0 < I_c$. If the linear extrapolation would hold to $E = 0$, this would mean that in the absence of impinging energy it would be possible to record a detection event with probability 0.01 if the detector was biased with $I_b = I_o$, which is not observed in experiments. A preliminary observation of nonlinearity in NbN has recently been reported.[45]

At present, there are two models that are consistent with our data: the model based on the time-dependent Ginzburg–Landau equation[44] and the model based on the dynamics of quasiparticle recombination.[33] The gain times length (GL) model takes a hotspot of fixed size as its initial condition, and the quasiparticle recombination model takes an area of uniformly suppressed superconductivity as its starting point. It is therefore not surprising that these descriptions work well for WSi, where the hotspot is known[30] to be larger than in NbN and comparable with the width of the wire.

The GL-model has the attractive feature that the detection is triggered by the movement of vortices. This ingredient was found to be crucial for explaining the behavior of NbN devices, because it introduces a dependence on the absorption position, which causes the position-dependent detection efficiency which we demonstrated recently.[19] On the other hand, we find no evidence of the low-current detection cutoff, which is predicted by the latest version of this model.[46] More experimental work is needed to determine the detection mechanism in WSi. In particular, it would be interesting to see if WSi has a position dependence, since this would answer the question regarding the role of vortices in the detection mechanism.

We investigated the detection mechanism in WSi SSPDs. We find that the bias current required to obtain a detection event depends only on the overall excitation energy, not on how that energy is distributed over a number of photons. At high photon energies, we observe a linear dependence between bias current and photon energy required to obtain a detection event. We find that, despite predictions of a normal hotspot in WSi, the square root form of the current–energy relation which is characteristic for some normal-core hotspot models is strongly excluded by our data. We find surprisingly strong similarities between our experimental results on WSi and previous results on NbN.

FIG. 3. The bias current required to trigger a detection with 0.01 probability is plotted as a function of total energy E_t for the 11 wavelengths. The error bars are reported together with data points and range between 2 nA and 90 nA. The different symbols belong to different detection regimes while each color corresponds to a wavelength. The red dotted circle highlights the overlap between 2-photon data point for $\lambda = 1100\,\text{nm}$ and the 3-photon data point for $\lambda = 1650\,\text{nm}$. The black dashed line results from a linear fit to the data points with $E_t > 0.8\,\text{eV}$ using the expression $I_b^{th} = I_o - \gamma E_t$. Inset: Zoom-in of the upper part of the graph. The data are represented by points to highlight the error bars.

[1] G. Goltsman, O. Okunev, G. Chulkova, A. Lipatov, A. Semenov, K. Smirnov, B. Voronov, A. Dzardanov, C. Williams, and R. Sobolewski, Appl. Phys. Lett. **79**, 705 (2001).

[2] C. M. Natarajan, M. G. Tanner, and R. H. Hadfield, Supercond. Sci. Technol. **25**, 063001 (2012).

[3] H. Takesue, S. W. Nam, Q. Zhang, R. H. Hadfield, T. Honjo, K. Tamaki, and Y. Yamamoto, Nat. Photonics **1**, 343 (2007).

[4] C. Zinoni, B. Alloing, L. H. Li, F. Marsili, A. Fiore, L. Lunghi, A. Gerardino, Yu. B. Vakhtomin, K. V. Smirnov, and G. N. Gol'tsman, Appl. Phys. Lett. **91**, 031106 (2007).

[5] D. Bitauld, F. Marsili, A. Gaggero, F. Mattioli, R. Leoni, S. Jahanmiri Nejad, F. Levy, and A. Fiore, Nano Lett. **10**, 2977 (2010).

[6] M. Shaw, K. Birnbaum, M. Cheng, M. Srinivasan, K. Quirk, J. Kovalik, A. Biswas, A. D. Beyer, F. Marsili, V. Verma, R. P. Mirin, S. W. Nam, J. A. Stern, and W. H. Farr, CLEO: Science and Innovations, SM4J. 2 (2014).

[7] A. J. Kerman, E. A. Dauler, J. K. W. Yang, K. M. Rosfjord, V. Anant, K. K. Berggren, G. N. Goltsman, and B. Voronov, Appl. Phys. Lett. **90**, 101110 (2007).

[8] R. Gaudio, K. M. P. op't Hoog, Z. Zhou, D. Sahin, and A. Fiore, Appl. Phys. Lett. **105**, 222602 (2014).

[9] T. Yamashita, S. Miki, H. Terai, and Z. Wang, Opt. Express **21**, 27177 (2013).

[10] D. Rosenberg, A. J. Kerman, R. J. Molnar, and E. A. Dauler, Opt. Express **21**, 1440–1447 (2013).

[11] B. Baek, A. E. Lita, V. Verma, and S. W. Nam, Appl. Phys. Lett. **98**, 251105 (2011).

[12] V. B. Verma, F. Marsili, S. Harrington, A. E. Lita, R. P. Mirin, and S. W. Nam, Appl. Phys. Lett. **101**, 251114 (2012).

[13] V. B. Verma, B. Korzh, F. Bussières, R. D. Horansky, A. E. Lita, F. Marsili, M. D. Shaw, H. Zbinden, R. P. Mirin, and S. W. Nam, Appl. Phys. Lett. **105**, 122601 (2014).

[14] F. Marsili, V. B. Verma, J. A. Stern, S. Harrington, A. E. Lita, T. Gerrits, I. Vayshenker, B. Baek, M. D. Shaw, R. P. Mirin, and S. W. Nam, Nat. Photonics **7**, 210 (2013).

[15] Y. P. Korneeva, M. Y. Mikhailov, Y. P. Pershin, N. N. Manova, A. V. Divochiy, Y. B. Vakhtomin, A. A. Korneev, K. V. Smirnov, A. G. Sivakov, A. Y. Devizenko, and G. N. Goltsman, Supercond. Sci. Technol. **27**, 095012 (2014).

[16] V. Verma, A. Lita, M. R. Vissers, F. Marsili, D. P. Pappas, R. P. Mirin, and S. W. Nam, CLEO QELS Fundamental Science FM3A 7 (2014).

[17] V. B. Verma, R. Horansky, F. Marsili, J. A. Stern, M. D. Shaw, A. E. Lita, R. P. Mirin, and S. W. Nam, Appl. Phys. Lett. **104**, 051115 (2014).

[18] J. J. Renema, R. Gaudio, Q. Wang, Z. Zhou, A. Gaggero, F. Mattioli, R. Leoni, D. Sahin, M. J. A. de Dood, A. Fiore, and M. P. van Exter, Phys. Rev. Lett. **112**, 117604 (2014).

[19] J. J. Renema, Q. Wang, R. Gaudio, I. Komen, K. op't Hoog, D. Sahin, A. Schilling, M. P. van Exter, A. Fiore, A. Engel, and M. J. A. de Dood, Nano Lett. **15**, 4541 (2015).

[20] A. Semenov, A. Engel, H. W. Hübers, K. Il'in, and M. Siegel, Eur. Phys. J. B **47**, 495 (2005).

[21] L. N. Bulaevskii, M. J. Graf, C. D. Batista, and V. G. Kogan, Phys. Rev. B **83**, 144526 (2011).

[22] L. N. Bulaevskii, M. J. Graf, and V. G. Kogan, Phys. Rev. B **85**, 014505 (2012).

[23] A. D. Semenov, G. N. Goltsman, and A. A. Korneev, Phys. C **351**, 349 (2001).

[24] A. Semenov, B. Günther, U. Böttger, H.-W. Hübers, H. Bartolf, A. Engel, A. Schilling, K. Ilin, M. Siegel, R. Schneider, D. Gerthsen, and N. A. Gippius, Phys. Rev. B **80**, 054510 (2009).

[25] H. Bartolf, A. Engel, A. Schilling, K. Il'in, M. Siegel, H.-W. Hübers, and A. Semenov, Phys. Rev. B **81**, 024502 (2010).

[26] S. P. Chockalingam, M. Chand, J. Jesudasan, V. Tripathi, and P. Raychaudhuri, Phys. Rev. B **77**, 214503 (2008).

[27] The values quoted here for WSi are for films produced at NIST.

[28] S. Kondo, J. Mater. Res. **7**, 853 (1992).

[29] A. Engel, J. Lonsky, X. Zhang, and A. Schilling, IEEE Trans. Appl. Supercond. **25**, 2200407 (2015).

[30] F. Marsili, M. J. Stevens, A. Kozorezov, V. B. Verma, C. Lambert, J. A. Stern, R. Horansky, S. Dyer, S. Duff, D. P. Pappas *et al.*, Phys. Rev. B **93**, 094518 (2016).

[31] Z. Zhou, G. Frucci, F. Mattioli, A. Gaggero, R. Leoni, S. Jahanmirinejad, T. B. Hoang, and A. Fiore, Phys. Rev. Lett. **110**, 133605 (2013).

[32] Z. Zhou, "*Multiphoton Detection with Superconducting Nanowires,*" PhD thesis, Eindhoven University of Technology, 2014.

[33] A. G. Kozorezov, C. Lambert, F. Marsili, M. J. Stevens, V. B. Verma, J. A. Stern, R. Horansky, S. Dyer, S. Duff, D. P. Pappas, A. Lita, M. D. Shaw, R. P. Mirin, and S. W. Nam, Phys. Rev. B **92**, 064504 (2015).

[34] J. S. Lundeen, A. Feito, H. Coldenstrodt-Ronge, K. L. Pregnell, C. Silberhorn, T. C. Ralph, J. Eisert, M. B. Plenio, and I. A. Walmsley, Nat. Phys. **5**, 27 (2009).

[35] J. J. Renema, G. Frucci, Z. Zhou, F. Mattioli, A. Gaggero, R. Leoni, M. J. A. d. Dood, A. Fiore, and M. P. van Exter, Opt. Express **20**, 2806 (2012).

[36] J. J. Renema, G. Frucci, Z. Zhou, F. Mattioli, A. Gaggero, R. Leoni, M. J. A. de Dood, A. Fiore, and M. P. van Exter, Phys. Rev. B **87**, 174526 (2013).

[37] A. Engel, J. J. Renema, K. Il'in, and A. Semenov, Supercond. Sci. Technol. **28**, 114003 (2015).

[38] See supplementary material at http://dx.doi.org/10.1063/1.4958687 for more details of the fabrication.

[39] The use of trade names is intended to allow the measurements to be appropriately interpreted, and does not imply endorsement by the US government, nor does it imply these are necessarily the best available for the purpose used here.

[40] J. J. Renema, R. Gaudio, Q. Wang, Z. Zhou, A. Gaggero, F. Mattioli, R. Leoni, D. Sahin, M. P. van Exter, A. Fiore, and M. J. A. de Dood, "Probing the Hotspot Interaction Length in NbN Nanowire Superconducting Single-Photon Detectors," preprint arXiv:1607.03088.

[41] Q. Wang, J. J. Renema, A. Gaggero, F. Mattioli, R. Leoni, M. P. van Exter, and M. J. A. de Dood, J. Appl. Phys. **118**, 134501 (2015).

[42] R. Lusche, A. Semenov, K. Ilin, M. Siegel, Y. Korneeva, A. Trifonov, A. Korneev, G. Goltsman, D. Vodolazov, and H.-W. Hübers, J. Appl. Phys. **116**, 043906 (2014).

[43] J. J. Renema, "*The Physics of Nanowire Superconducting Single-Photon Detectors,*" PhD thesis, Leiden University, 2015.

[44] D. Yu. Vodolazov, Phys. Rev. B **90**, 054515 (2014).

[45] D. Yu. Vodolazov, Yu. P. Korneeva, A. V. Semenov, A. A. Korneev, and G. N. Goltsman, Phys. Rev. B **92**, 104503 (2015).

[46] D. Yu. Vodolazov, private communication (2016).